Available online at www.sciencedirect.com
SCIENCE DIRECT®
Developmental Biology 268 (2004) 295–311
DEVELOPMENTAL BIOLOGY
www.elsevier.com/locate/ydbio

Signaling through Gsα is required for the growth and function of neuromuscular synapses in *Drosophila*

William J. Wolfgang,[a,1] Catherine Clay,[a] Jacqueline Parker,[a] Ricardo Delgado,[b] Pedro Labarca,[b] Yoshiaki Kidokoro,[c] and Michael Forte[a,*]

[a] *Vollum Institute, Oregon Health and Science University, Portland, OR 97239, USA*
[b] *Centro de Estudio Cientificos, Valdivia, Chile*
[c] *Gunma University School of Medicine, Maebashi 371-8511, Japan*

Received for publication 5 September 2003, revised 5 January 2004, accepted 9 January 2004

Abstract

Although synapses are assembled in a highly regulated fashion, synapses once formed are not static structures but continue to expand and retract throughout the life of an organism. One second messenger that has been demonstrated to play a critical role in synaptic growth and function is cAMP. Here, we have tested the idea that signaling through the heterotrimeric G protein, Gs, plays a coincident role with increases in intracellular Ca^{+2} in the regulation of adenylyl cyclases (ACs) during synaptic growth and in the function of synapses. In larvae containing a hypomorphic mutation in the *dgs* gene encoding the *Drosophila* Gsα protein, there is a significant decrease in the number of synaptic boutons and extent of synaptic arborization, as well as defects in the facilitation of synaptic transmission. Microscopic analysis confirmed that Gsα is localized at synapses both pre- and postsynaptically. Restricted expression of wild-type Gsα either pre- or postsynaptically rescued the mutational defects in bouton formation and defects in the facilitation of synaptic transmission, indicating that pathways activated by Gsα are likely to be involved in the reciprocal interactions between pre- and postsynaptic cells required for the development of mature synapses. In addition, this Gsα mutation interacted with *fasII*, *dnc*, and hyperexcitability mutants in a manner that revealed a coincident role for Gsα in the regulation of cAMP and FASII levels required during growth of these synapses. Our results demonstrate that Gsα-dependent signaling plays a role in the dynamic cellular reorganization that underlies synaptic growth.

Keywords: Gsα; Synaptic growth; cAMP; *Drosophila*; Signaling

Introduction

Although synapses are assembled in a highly regulated fashion, once formed, they are not static structures but continue to expand and retract throughout the life of an organism. This process of dynamic reorganization is thought to underlie complex neuronal functions including learning and memory and depends on a variety of evolutionarily conserved mechanisms that coordinate the growth and activity of pre- and postsynaptic cells (Cohen-Cory, 2002; Woolf and Salter, 2000). Of the many transduction pathways known to be involved in modulating this process, one critical and conserved component of every form of synaptic growth examined involves the second messenger, cAMP (Davis and Goodman, 1998; Martin and Kandel, 1996).

In *Drosophila*, processes regulating synaptic expansion have been revealed by examining the consequences of mutations in genes that define specific biochemical processes on the formation of larval neuromuscular junctions (NMJ), thus implicating each in the control of synaptic growth (Keshishian et al., 1996; Koh et al., 2000). The functions identified by many of these mutations have also been shown to play a critical role in the development of synapses in a number of other systems (Elgersma and Silva, 1999; Koh et al., 1999). The role of cAMP in *Drosophila* NMJ growth emerged from an analysis of larvae containing mutations in genes that control neuronal electrical activity and cAMP levels. From these studies, a model was developed in which neuronal activity leads to elevated intracel-

* Corresponding author. Vollum Institute, L474, Oregon Health and Science University, 3181 S.W. Sam Jackson Park Road, Portland, OR 97239. Fax: +1-503-494-4976.
E-mail address: forte@ohsu.edu (M. Forte).
[1] Present address: David Axelrod Institute, 120 New Scotland Ave., Albany NY 12208, USA.

0012-1606/$ - see front matter © 2004 Elsevier Inc. All rights reserved.
doi:10.1016/j.ydbio.2004.01.007

lular Ca^{+2} through activation of voltage-dependent Ca^{+2} channels; increases in intracellular Ca^{+2} lead to activation of Ca^{+2}-calmodulin-regulated adenylyl cyclases (ACs) and elevation of intracellular cAMP. Downstream processes regulated by cAMP appear to mediate their effects through down-regulation of the levels of the homophilic cell adhesion molecule (CAMs), FASII, which normally acts to restrain synaptic growth (Schuster et al., 1996a,b).

In addition to responding to Ca^{+2} signals, ACs are also activated by the heterotrimeric G protein, Gs. While all isoforms of AC identified so far are stimulated by the GTP-bound form of the α-subunit of Gs (Gsα) (Cooper et al., 1998; Smit and Iyengar, 1998; Taussig and Zimmermann, 1998), biochemical characterization of mammalian Ca^{+2}-calmodulin-regulated ACs (e.g., AC1) has demonstrated that simultaneous elevation of Ca^{+2} and activation by Gs following receptor activation result in cAMP levels many folds higher than is possible by either stimulus alone (Impey et al., 1994; Wayman et al., 1994). Since Ca^{+2}-calmodulin-regulated ACs are important coincidence detectors, it is reasonable to predict then that both activity-dependent (i.e., Ca^{+2}-mediated) and receptor-dependent (i.e., Gsα-mediated) modulation of ACs may be required to establish correct levels of cAMP for appropriate synaptic growth. To test the role of Gsα signaling in synaptic growth and function, we have taken advantage of the fact that all receptor-mediated pathways for AC activation require Gsα. This work is motivated by previous studies that have shown that alterations in Gsα signaling, either in larvae carrying mutations in the *dgs* gene encoding Gsα or by expression of gain-of-function forms of this protein, result in predicted alterations in the levels of cAMP and profound behavioral defects, suggestive of alterations in synaptic transmission and plasticity (Chyb et al., 1999; Connolly et al., 1996; Wolfgang et al., 2001). Consequently, in this report, we investigate NMJ development and synaptic activity in larvae containing a hypomorphic mutation in the gene encoding the *Drosophila* Gsα protein. Our results demonstrate that Gsα-dependent signaling plays a role in processes that underlie synaptic growth.

Materials and methods

Fly stocks

The dgs^{R60} null, dgs^{B19} hypomorphic mutation, *Gs27* transgene, and flies containing *UAS-wtGsα*, *UAS-wtGiα*, and *UAS-HA*-tagged *wtGsα* constructs have been described (Li et al., 2000; Wolfgang et al., 1996, 2001). $Df(2R)or^{BR\text{-}11}$ cn^1 bw^1 $sp^1/SM6A$, dnc^1, and GFP balancer stocks were supplied by the Bloomington Stock Center. GAL4 drivers $elav^{3A4}$*-GAL4*, *MHC82-GAL4*, and *B185-GAL4*, which mediate expression throughout the CNS, muscles, and motoneurons and muscles, respectively (Davis et al., 1997; Schuster et al., 1996a), were provided by Dr. G. Davis. GAL4 drivers *C57-GAL4* and *C380-GAL4*, which mediate expression in muscle and motoneurons, respectively (Budnik et al., 1996), as well as eag^1, Sh^{120}, and $dlg^{x\text{-}1}$ mutants, were provided by Dr. V. Budnik. Stocks containing the $fasII^{e86}$ mutation were provided by Dr. C. Goodman, and rut^1 $f^1/FM7A$ stocks were provided by Dr. R. Davis.

Electrical recording

Nerve-evoked synaptic currents were recorded in third instar larvae using the two microelectrode voltage clamp techniques as described earlier (Acharya et al., 1998; Delgado et al., 1998). Longitudinal muscles 6 or 7 at abdominal segment A2 or A3 were used. The membrane potential was held at −80 mV. Experiments were carried out in a standard external solution, which had the following composition (in mM): NaCl, 128; KCl, 2; $MgCl_2$, 4; $CaCl_2$, 0.2; HEPES, 5; sucrose, 36 (pH 7.3). To change the Ca^{2+} concentration, required $CaCl_2$ was added to the external solution. For stimulation, the nerve was cut close to the ventral nerve cord and sucked into a pipette filled with the standard external saline. The nerve was stimulated at intensities intended to obtain maximal synaptic responses and at frequencies indicated in each experiment using a programmable stimulator (Master-8, A. M. P. I., Jerusalem, Israel). Data acquisition and analysis were performed using pClamp software (Axon Instruments, Foster City).

Immunohistochemistry

Wandering third instar larvae were collected from uncrowded vials that were maintained at 25 °C. For dissection, larvae were pinned out in Sylgard dishes and cut along the dorsal midline, and the internal organs, fat body, discs, major trachea, and brain were carefully removed. The larval preparations were subsequently fixed in 4% formaldehyde in phosphate-buffered saline (PBS) for 1 h at room temperature, washed three times over 1 h in PBS containing 10% horse serum and 0.3% Triton-X100 (blocking solution), and then incubated with specific antibodies overnight at 4 °C. Polyclonal antibodies to *Drosophila* synaptotagmin (1/2000; gift of Dr. H. Bellen), horseradish peroxidase (HRP, 1/1000; Capell), *discs-large* (1/1000; gift of V. Budnik), Gsα (1/500; Wolfgang et al., 1991), and monoclonal antibodies to FASII (1D4, 1/10; Developmental Studies Hybridoma Bank and C. Goodman) and the HA epitope (1/1000; Convance) were diluted in blocking solution. Antibody binding was detected using the HRP-based ABC Elite kit (Vector Labs) or with an appropriate secondary antibody coupled to either Alexa 488 (Molecular Probes), FITC, or Texas Red (Vector Labs). For duel label analysis, a stack of images for each fluorochrome was collected through the entire thickness of the synapse using a motorized Axiophot ll stage (Zeiss). The images where then deconvolved using Openlab software (Improvision). The final image is from a single layer of the deconvolved stack of images.

Quantification of bouton numbers and branching

Synaptic boutons were identified and quantified following staining with antibodies directed against *Drosophila* synaptotagmin. Larvae were examined at 40× using differential interference contrast optics. Boutons were counted on muscles 6 and 7 in each hemisegment of abdominal segment 2. Branches were defined as sections of neurites containing at least two boutons and extending from the principle axis of the synapse in muscles 6 and 7, which runs along the boundary between the two muscles. All data and statistical comparisons were made in Statview (SAS Inc., Cary, NC). Muscle size in mutant larvae was within the variation observed in the case of control larvae.

Quantification of FASII staining by confocal microscopy

From a *y f C(1)/Y/fasII^{e86}*, *cn^{1} bw^{1} dgs^{B19}/CyO-GFP* stock, the following genotypes were processed together in the same tube, mounted on the same slide, and imaged during a single session on the confocal microscope. The genotypes of the four larvae were *y f C(1)/Y, cn^{1} bw^{1} dgs^{B19}/CyO-GFP* females that served as controls; *fasII^{e86}, cn^{1} bw^{1} dgs^{B19}/CyO-GFP* males that served as single *fasII^{e86}* mutants; *y f C(1)/Y, cn^{1} bw^{1} dgs^{B19}/cn1 bw^{1} dgs^{B19}* females that served as single *dgs^{B19}* mutants; and *fasII^{e86}, cn^{1} bw^{1} dgs^{B19}/cn1 bw^{1} dgs^{B19}* males that served as *fasII^{e86}, dgs^{B19}* double mutants. The four types of larvae were dissected as previously described and fixed in 4% formaldehyde in PBS for 1 h, washed in blocking solution, and incubated with antibodies to FASII overnight at 4°C. Antibody binding was detected with Alexa 488-conjugated second antibody. The four larval types were then mounted on the same slide in an antifade solution of 50% glycerol containing 0.5 mg/ml p-phenylene-diamine. Neuromuscular synapses at muscles 6 and 7 and 12 and 13 for segments A2 through A5 were imaged with a BioRad Scanning Laser Confocal microscope at 3% power and 1500 gain. Under these conditions, there was no appreciable bleaching of the specimens.

The "synapse staining intensity" of individual synapses was determined in a manner similar to Thomas et al. (1997). Using the "plot profile" function of NIH image 1.61, the maximum intensity of a line drawn from the center of the synapse to past its outermost edge was measured. Four measurements for each synapse were made from lines drawn at approximately 45°, 135°, 225°, and 315° to the axis of the neurite traversing the synapse. From the average of these four measurements, the background level of staining, determined as the average intensity of a line drawn on the muscle adjacent to the NMJ being scored, was subtracted to determine the synapse staining intensity for a given synapse (Thomas et al., 1997).

To compare the synapse staining intensity between different genotypes and between animals imaged at different times, we calculated the index of intensity (*i*) for each synapse in the following manner. The synapse staining intensity between 40 and 60 synapses in the larvae of the control genotype on an individual slide was averaged. Then, for each synapse scored in both experimental and control larvae, the synapse's index of intensity (*i*) was determined by dividing that synapse's staining intensity by the average intensity of the control synapses on that slide. Thus, synapses from control animals have an average intensity index (*i*) of 1. Indexes less than one indicate reduced FASII staining compared to controls, while indexes greater than one reflect elevated levels of FASII compared to controls.

EM immunolocalization of Gsα

For EM studies, larvae were dissected as described above and fixed on ice in periodate–lysine–paraformaldehyde for 1 h, washed in PBS, and quenched for 5 min in PBS with 0.05 M glycine (McLean and Nakane, 1974). Larvae were then placed in EM blocking buffer containing 0.1% saponin and 10% horse serum in PBS for 1–4 h at room temperature, incubated overnight at 4°C with antibodies to Gsα diluted in blocking buffer (1/500), and then washed in three changes of blocking solution over 1 h at room temperature. Larvae were transferred to blocking solution containing anti-rabbit IgG FAB fragments conjugated to 1.4 nm of gold particles (1/100; Nanoprobes) for 1 h, washed again for 1 h in blocking solution, rinsed briefly in PBS, postfixed for 20 min in 1% glutaraldehyde, washed in blocking solution containing 0.05 M glycine, and finally washed in water. To detect the gold particles at the EM level, their size was increased to between 5 and 10 nm by incubation in Gold-enhance solution (Nanoprobes) for 5 min. The larvae were then rinsed briefly in cacodylate buffer, postfixed in 2% OsO_4, rinsed again in cacodylate buffer, incubated in 2% uranyl acetate for 30 min, and then dehydrated and embedded in epoxy for conventional EM preparation and viewing. Active zones are defined at the EM level as the synaptic region containing cortical electron dense material and constituting the site of vesicle release and neurotransmission (Sone et al., 2000).

Results

Synaptic defects generated by a mutation in dgs with reduced function

Previous characterization of null mutations in the gene encoding the *Drosophila* Gsα protein, *dgs*, indicated that the late embryonic–early larval lethality associated with these mutations is not associated with any striking morphologic abnormality (Wolfgang et al., 2001). Thus, lethality is likely due to the absence of an essential function mediated by Gsα during the initial stages of larval development rather than a requirement for this protein or the signaling pathway it modulates in any particular step during embryogenesis.

Immunocytochemical analysis of general neuromuscular development in embryos homozygous for *dgs*-null alleles using antibodies to HRP, FASII, or myosin heavy chain has shown that all stages of embryonic neuronal and muscle development proceed normally in mutant organisms (data not shown). In addition, the generation of null photoreceptor clones in the adult eye through mitotic recombination has demonstrated that axonal projections to the CNS are established normally in the absence of Gsα (data not shown). Thus, the Gsα protein and the pathway it defines are not

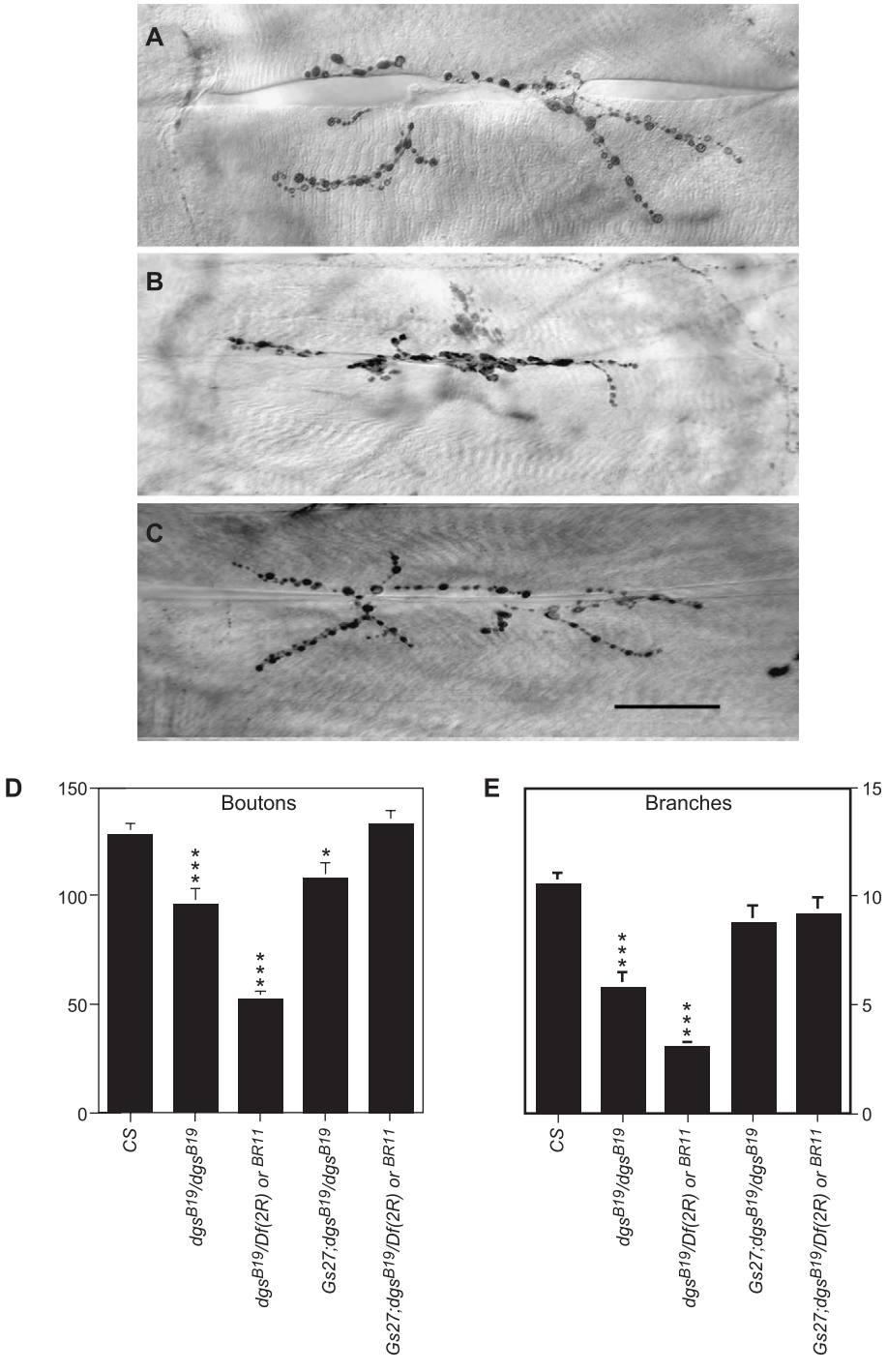

Fig. 1. Synaptic structure of NMJs and quantitation of the number of boutons and branches on muscles 6 and 7 in abdominal segment A2 from third instar, climbing stage larvae of various genotypes. (A) CS control; (B) w^1; cn^1 bw^1, dgs^{B19} (dgs^{B19} homozygotes); (C) *Gs27*; *cn bw* dgs^{B19}/*Df (2R)or*$^{BR-11}$ (rescued dgs^{B19} hemizygotes). All stained with antisynaptotagmin. (D) Quantitation of number of synaptic boutons and (E) extent of synaptic arborization. Asterisks indicate that the values are significantly different from CS controls. *Gs27* represents a *dgs* rescue transgene inserted on the X chromosome (Wolfgang et al., 2001). Note the reduced numbers of branches and synaptic boutons in dgs^{B19} homozygote and hemizygote mutants compared to control or rescued dgs^{B19} hemizygotes. Scale bar = 50 μm . *$p < 0.05$, **$p < 0.01$,***$p < 0.001$. $n = 15–20$.

likely to play an important role in patterning of the *Drosophila* embryo, in the elaboration of any specific embryonic structures such as the nervous system, or in processes involved in the cAMP-dependent regulation of growth cone guidance as suggested in vertebrate systems (e.g., Ming et al., 1997).

In contrast, the dgs^{B19} mutation is hypomorphic (reduced function, not absence of function) since homozygous, transheterozygous, and hemizygous mutants can survive up to the pupal stage. The amino acid change generated by this mutation, I373F, alters a C-terminal residue conserved in all Gsα proteins. Indeed, the C-terminal 41 amino acids in Gsα isoforms identified in *Caenorhabditis*, *Drosophila*, and mammals are completely conserved (Harris et al., 1985; Jansen et al., 1999; Quan et al., 1989). Numerous studies have identified this domain as essential not only for interactions between Gsα and receptors, but also for determining G protein-receptor specificity (e.g., Akhter et al., 1998; Conklin et al., 1996; Gilchrist et al., 1998, 1999; Mazzoni et al., 2000; Rasenick et al., 1994). Previous studies have also demonstrated that fly Gsα can couple receptors to the activation of ACs in cultured mammalian cell systems in which the expression of the endogenous Gsα protein was eliminated (Quan et al., 1991) and that cAMP levels are reduced in dgs^{B19} mutant larvae (Wolfgang et al., 2001). Thus, it is reasonable to conclude that the substitution generated by the dgs^{B19} mutation results in a reduction in receptor-Gsα interactions, leading to the hypomorphic phenotype. Consistent with this interpretation, maternally mutant dgs^{B19} embryos show similar levels and patterns of Gsα staining as heterozygous siblings (Wolfgang et al., 2001), suggesting that the dgs^{B19} phenotype is generated by expression of wild-type levels of a Gsα protein with reduced function. These earlier studies also demonstrated that larvae homozygous for dgs^{B19} are sluggish, not attracted to yeast granules, and show uncoordinated movements, indicating deficits in sensory-motor processes and raising the possibility that dgs^{B19} larvae have defects in neuromuscular function. To examine this issue in greater detail, we assessed muscle innervation in *Drosophila* third instar larvae containing the dgs^{B19} mutation.

Each hemisegment (abdominal segments A2–A7) of third instar larvae contains a stereotyped pattern of 30 muscles. We focused our analysis on muscles 6 and 7 in A2, which are innervated by two glutamatergic motor neurons that form type I terminals (Budnik, 1996; Keshishian et al., 1996). We visualized the overall pattern of innervation by immunostaining with anti-HRP, which specifically labels all insect neurons (Jan and Jan, 1982), and quantified the numbers of boutons and neuronal branching by immunostaining with antisynaptotagmin, a component of the exocytotic machinery that identifies synaptic vesicles. We found that although the overall pattern of innervation was normal, the number of synaptic boutons was significantly decreased in wandering stage dgs^{B19}/dgs^{B19} third instar larvae, which contain two copies of the hypomorphic dgs^{B19} allele (dgs^{B19} homozygotes) (Fig. 1). Bouton numbers were further decreased in $dgs^{B19}/Df(2R)or^{BR\text{-}11}$ larvae, which contain one copy of the dgs^{B19} allele [dgs^{B19} hemizygotes; $Df(2R)or^{BR\text{-}11}$ is a deletion of the genomic region containing the *dgs* gene]. Decreased numbers of boutons were associated with a significant decrease in the extent of synaptic arborization in dgs^{B19} homozygous larvae, which was also further decreased in dgs^{B19} hemizygous larvae (Fig. 1). In dgs^{B19} homozygous and hemizygous larvae, the reduction in branching and bouton number was restored to wild-type levels or partially restored to wild-type levels by introduction of one copy of a transgene encoding of the wild-type *dgs* gene. These observations implicate a role for Gsα-mediated signaling in the regulation of synaptic expansion during larval growth.

To assess the developmental time course of the appearance of defects in dgs^{B19} mutants, we examined NMJ phenotypes at earlier developmental stages. As shown in Table 1, while the extent of synaptic branching in dgs^{B19} mutants was slightly reduced in late second instar stages, the number of synaptic boutons formed in mutant second instar larvae was not significantly different from that observed in wild-type controls (Table 1). Furthermore, immunocytochemical analysis using antibodies to HRP, FASII, a marker for the peripheral nervous system (Mab 22C10), or myosin heavy chain demonstrated that neuronal and muscle development proceeded normally during all embryonic and larval stages (data not shown). When compared with the results shown in Fig. 1, these data suggest then that defects in NMJ formation only become apparent in *dgs* mutants during the third instar stages, the period of greatest muscle expansion and ensuing addition of NMJs. These observations are consistent with the idea that signaling through Gsα specifically contributes to the ability of neurons to form new synapses and branches as the muscle grows.

Impaired synaptic plasticity in dgs^{B19} mutant larvae

To assess the physiologic consequences of the dgs^{B19} mutation, we examined synaptic transmission in mutant larvae using standard electrophysiologic techniques. When the nerve was stimulated at 0.3 Hz, the average amplitudes of synaptic currents in control and homozygous dgs^{B19} mutant larvae were dependent on the external Ca^{+2} concentration, as it was in control larvae, but were not significantly different between mutant and control larvae at Ca^{+2} concentrations ranging from 0.1 to 0.3 mM (Fig. 2A). Since

Table 1
Quantification of boutons and branches in dgs^{B19} second instar larvae

Genotype	Boutons ± SE	Branches ± SE	*n*
Control	34 ± 7.5	6.7 ± 0.67	6
dgs^{B19}	35 ± 2	4.9 ± 0.38	15
P	0.86	0.02	

n = number of hemisegments scored. Control represents CantonS larvae.

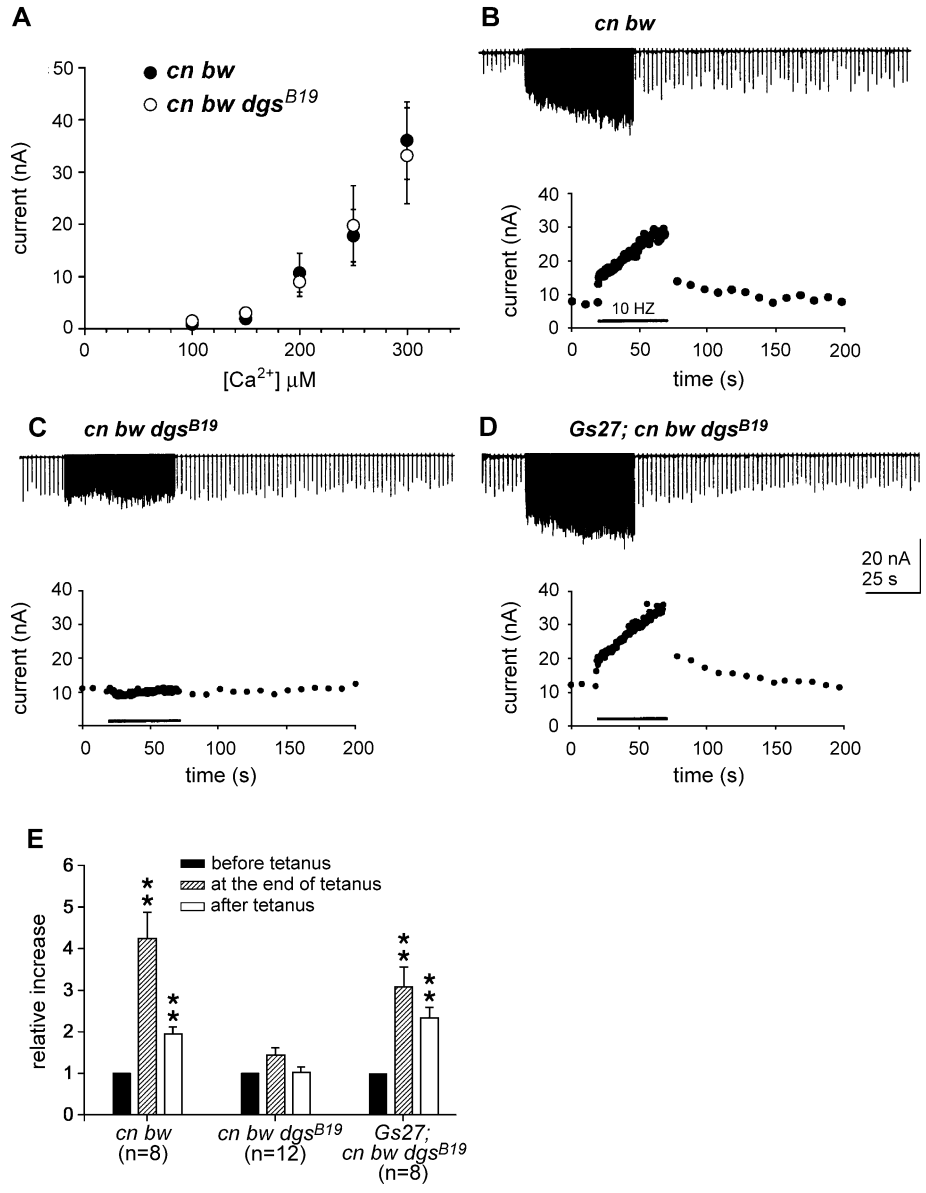

Fig. 2. Nerve-evoked synaptic currents in dgs^{B19} larvae and controls. (A) The mean amplitude of synaptic currents versus external Ca^{2+}. The mean amplitude of 10 consecutive synaptic currents evoked with stimulation at 0.3 Hz is plotted against external Ca^{2+} concentration (μM) for w^1; cn^1 bw^1, dgs^{B19} mutant larvae (○) and for control, cn^1 bw^1 (●). (B–D) Sample traces of synaptic currents during tetanus experiments in external solutions containing 0.2 mM Ca^{2+}. The nerve was first stimulated at 0.3 Hz, then switched to 10 Hz for 50 s (tetanus), and finally returned to 0.3 Hz. The upper trace in each panel is a synaptic current trace under voltage clamp. The lower graph is a plot of average amplitude of three consecutive synaptic currents before, during, and after tetanus against time. The horizontal bar above the abscissa indicates the timing and duration of tetanus. (B) cn^1 bw^1 control. (C) cn^1 bw^1, dgs^{B19} homozygotes. (D) w^1, $Gs27^1$; cn^1 bw^1, dgs^{B19} (dgs^{B19} homozygotes containing the *Gs27* rescue transgene). Calibration bars in D apply to all current traces. (E) Summary of the results of tetanic stimulation. Three columns for each set correspond to the mean amplitude of 10 consecutive synaptic currents before tetanus (solid column), at the end of tetanus (hatched column), and immediately after tetanus (unshaded column). Genotypes indicated below each set of bars. The mean amplitudes during tetanus and after tetanus were normalized to that before tetanus. Asterisks indicate that the values are significantly different from controls (*$p < 0.05$, **$p < 0.01$).

smaller muscles have smaller synaptic currents, this finding also indicates that muscles are not detectably smaller than controls in dgs^{B19} mutants. In the slope of the double logarithmic plot, the apparent cooperativity, n, was 3.9 ± 0.4 ($n = 5$) for dgs^{B19} mutant larvae and 3.6 ± 0.2 ($n = 5$) for control larvae. When the stimulus frequency was increased to 10 Hz for 50 s, the amplitude of synaptic currents in control larvae (Fig. 2B) increased during tetanic stimulation (facilitation during tetanus) and remained increased after tetanus for approximately 1 min [posttetanic potentiation (PTP)]. In contrast, in dgs^{B19} homozygous larvae, the amplitude of synaptic currents did not increase either during or immediately after tetanic stimulation (Fig. 2C). Introduction of one copy of a transgene containing the wild-type *dgs* gene (Gs27) into the dgs^{B19} mutant background rescued the defects in facilitation of synaptic transmission during teta-

nus and posttetanic potentiation to that observed in controls (Fig. 2D), demonstrating that these defects in the plastic properties of synaptic transmission are due to the dgs^{B19} mutation. To quantify the extent of synaptic facilitation during tetanus and posttetanus, the mean amplitude of last 10 synaptic currents during tetanus and that of first 10 synaptic currents after tetanus were normalized to that before tetanus. These values were then compared among mutant and control larvae. Both parameters in the mutant larvae were significantly smaller than observed in the control and were returned to control levels by introduction of the rescue transgene (Fig. 2E).

Localization of Gsα at forming neuromuscular junctions

Although Gsα has been previously shown to be widely distributed in embryos and to be enriched in the CNS at all developmental stages, we examined the distribution of Gsα specifically at the NMJ of late third instar larvae using immunocytochemical techniques. Gsα is localized in NMJs of both control (Fig. 3A) and dgs^{B19} mutants (Fig. 3B) in a diffuse halo around each synapse. Immunolocalization at the EM level revealed that the majority of Gsα immunoreactivity is associated with the subsynaptic reticulum (SSR), with substantially lower levels present in the presynaptic nerve terminal (Fig. 3C). At the EM level, Gsα immunoreactivity does not appear to be concentrated in one region of the synapse in either the pre- or postsynaptic cell, although in the SSR, Gsα appears to be mostly associated with the plasma membrane. Gsα is also associated with the sarcolemma (data not shown). To further confirm the pre- and postsynaptic localization of Gsα at larval NMJs, we took advantage of UAS transgenes that direct the expression of HA-tagged forms of wild-type Gsα (Wolfgang et al., 1996). Restricted expression of tagged forms of Gsα, as mediated by either MHC82-GAL4 driver (muscle or postsynaptic) or the elav-GAL4 driver (neuron or presynaptic), followed by immunostaining of synapses with an antibody directed to the HA epitope, clearly demonstrated the complementary pre- and postsynaptic localization of Gsα (Figs. 3D and E).

Recently, it has been proposed that neurotransmission and synaptic growth are regulated in two discrete subcellular synaptic compartments: (1) the active zone, defined at the EM level as the synaptic region containing cortical electron dense material and constituting the site of vesicle release and neurotransmission; and (2) the periactive zone, which surrounds the active zone (Chang and Balice-Gordon, 2000;

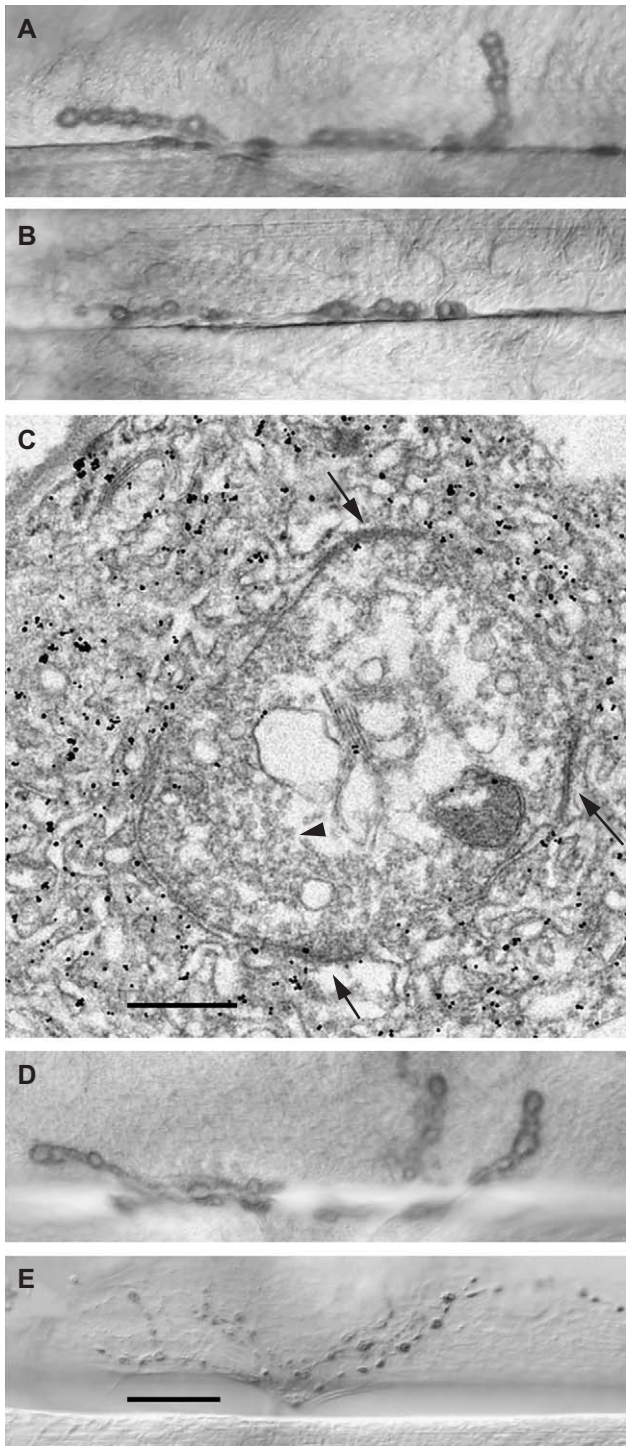

Fig. 3. Localization of Gsα at NMJs in muscles 6 and 7. (A) Light level micrograph of Gsα in a CS control and (B) w^1; cn^1, bw^1, dgs^{B19} homozygote. Note that in both cases, the distribution of Gsα appears as a halo at the synaptic terminals. (C) EM immunolocalization of endogenous Gsα in a wild-type (CS) NMJ. Gold particles are almost exclusively confined to the postsynaptic subsynaptic reticulum (SSR) with only the occasional gold particle localized presynaptically. Gold particles were not strongly associated with synaptic densities but appear relatively uniformly distributed throughout the SSR. Immunoreactivity was generally excluded from mitochondria and the myofibrillar portion of the muscle cell. Gold particles are also present on the sarcolemma outside of the SSR. Scale bar = 0.5 μm. Arrows indicate synaptic densities, and arrow heads indicate synaptic vesicles. (D and E) NMJs in wild-type larvae following pre- or postsynaptic expression of wild-type, HA-tagged Gsα and staining with an antibody directed to the HA epitope. (D) Expression of wild-type, HA-tagged Gsα postsynaptically using the MHC82-GAL4 driver. (E) Expression of wild-type, HA-tagged Gsα presynaptically using the elav-GAL4 driver. Scale bar in E = 30 μM and applies to A, B, D, and E.

Sone et al., 2000). At the light microscopic level, these spatial subdomains have been defined by the discrete localization of specific proteins such as FASII and the product of the *discs-large* gene (DLG). Thus, we compared the distribution of Gsα within synapses to each of these marker proteins.

FASII is expressed both pre- and postsynaptically, is required in both cells for proper growth of NMJs, and at the EM level is concentrated at the boundary between these two cells. In light level images, FASII is absent from the active zone and present in the periactive zone (Chang and Balice-Gordon, 2000; Sone et al., 2000). Coimmunostaining with FASII and Gsα antibodies shows that Gsα immunoreactivity can be seen in regions that are devoid of FASII staining (arrows, Fig. 4C), indicating that Gsα is present in synaptic active zones (pre- or postsynaptic localization cannot be determined in these light level images). Gsα overlaps with FASII and thus is present in the periactive zone. Finally, Gsα expression extends past the extent of FASII staining in the SSR and is also detected on the sarcolemma (data not shown).

The DLG protein, which is largely distributed postsynaptically in the SSR, coordinates the localization of a number of molecules within synapses, including FASII and Shaker potassium channels (Budnik et al., 1996; Lahey et al., 1994; Tejedor et al., 1997), and is also required for proper NMJ formation (Budnik et al., 1996; Lahey et al., 1994). Colocalization of DLG and Gsα shows that in the more proximal regions of the SSR (as defined by DLG staining), the two proteins are expressed in overlapping domains (Fig. 4F). However, in the more distal regions away from sites of direct contact between nerve and muscle, Gsα is present in regions devoid of DLG.

We also assessed whether colocalization of Gsα with DLG is dependent on DLG by examining the localization of Gsα in larvae containing the strong *dlg* mutation, $dlg^{X\text{-}1}$ (Thomas et al., 1997). Gsα localization was not dramatically altered by this *dlg* mutation or by mutations in other proteins known to be involved in the localization of protein complexes at NMJs, *scribble* (Bilder and Perrimon, 2000; Roche et al., 2002), *guk-holder* (Mathew et al., 2002), and *lethal giant larvae* (Bilder et al., 2000; Peng et al., 2000) (data not shown). In addition, the localization of both DLG and FASII appeared unchanged from wild type in dgs^{B19} mutant larvae (data not shown). Thus, the Gsα protein occupies a unique domain within synapses when compared to DLG and FASII;

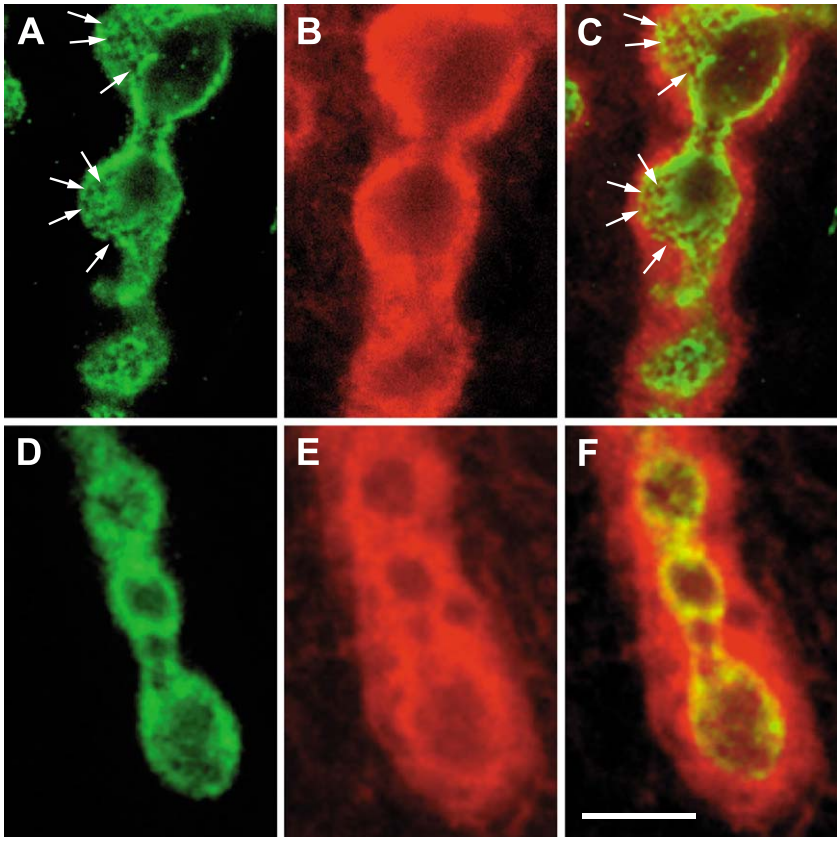

Fig. 4. Colocalization of Gsα with either FASII (A–C) or DLG (D–F) in synapses of wild-type CS larvae. The absence of FASII staining (A, green) defines active zones (Chang and Balice-Gordon, 2000; Sone et al., 2000). Gsα (B, red) and merged image (C) are present in regions devoid of FASII staining and throughout a wider area of the SSR or sarcolemma. DLG (D, green) always colocalizes with Gsα (E, red, and F, merged image), but again Gsα extends further into the SSR or sarcolemma than DLG. Arrows indicate active zones in A and C. Scale bar = 2.5 μm.

Gsα is associated with regions devoid of FASII staining, yet Gsα is also present in domains that extend past those associated with FASII and DLG staining. Moreover, the localization of Gsα at the NMJ appears not to be dependent on mechanisms regulating the localization of other synaptic proteins examined in this study.

Expression of Gsα in nerve and/or muscle rescues NMJ defects present in dgs^{B19} mutants

To determine the contribution of pre- and postsynaptic expression of Gsα with respect to the generation of the NMJ defects present in dgs^{B19} larvae, we used the GAL4-UAS system to drive expression of wild-type Gsα in specific patterns in third instar larvae (Brand and Perrimon, 1993; Brand et al., 1994). Initially, we took advantage of the fact that the B185-GAL4 drives expression in both nerves and muscles (Davis et al., 1997; Schuster et al., 1996b) during this stage. Larvae carrying the dgs^{B19} mutation and B185-GAL4 driving expression of Gsα restored NMJ arborization and bouton numbers to wild-type levels (Figs. 5B and 6A and B). We then asked if restricted expression of Gsα in either nerves or muscles alone would be sufficient to rescue the NMJ defects present in dgs^{B19} homozygotes. To mediate expression in neurons, pan-neural expression in embryos and larvae was driven by use of the elav-GAL4 driver; alternatively, expression was restricted to motor neurons by use of the C380-GAL4 insertion. To assess whether muscle-specific expression could rescue neuromuscular defects present in dgs^{B19} homozygotes, expression of Gsα was mediated by the muscle-specific drivers, MHC82-GAL4 and C57-GAL4. The morphology of NMJs in each case was rescued to that seen in wild-type larvae (Figs. 5C and D). Quantitation of synaptic arborization and bouton number confirmed that directed expression of Gsα throughout the CNS (elav-GAL4) or specifically in motor neurons (C380-GAL4) is sufficient to rescue the defects in synaptic branching and bouton formation present in dgs^{B19} homozygotes relative to controls [e.g., dgs^{B19} homozygotes and dgs^{B19} homozygote containing UAS-wtGsα alone (Figs. 5E and 6A and B) or GAL4 drivers alone (data not shown)]. Furthermore, restricted expression of Gsα in muscle as mediated by either the C57-GAL4 driver or the MHC82-GAL4 driver is sufficient to rescue the dgs^{B19}-mediated defects in bouton formation relative to controls, while muscle-specific expression was only able to partially rescue the branching defects observed in dgs^{B19} mutants (Figs. 6A and B). In addition, either pre- or postsynaptic expression of Gsα was also able to rescue the defects in facilitation of synaptic transmission during tetanus and posttetanic facilitation that was observed in dgs^{B19} mutants (Fig. 6C). In all cases mentioned above, restricted expression of Gsα in both nerve and muscle of wild-type larvae using the B185-GAL4 driver or expression in either nerve or muscle alone of wild-

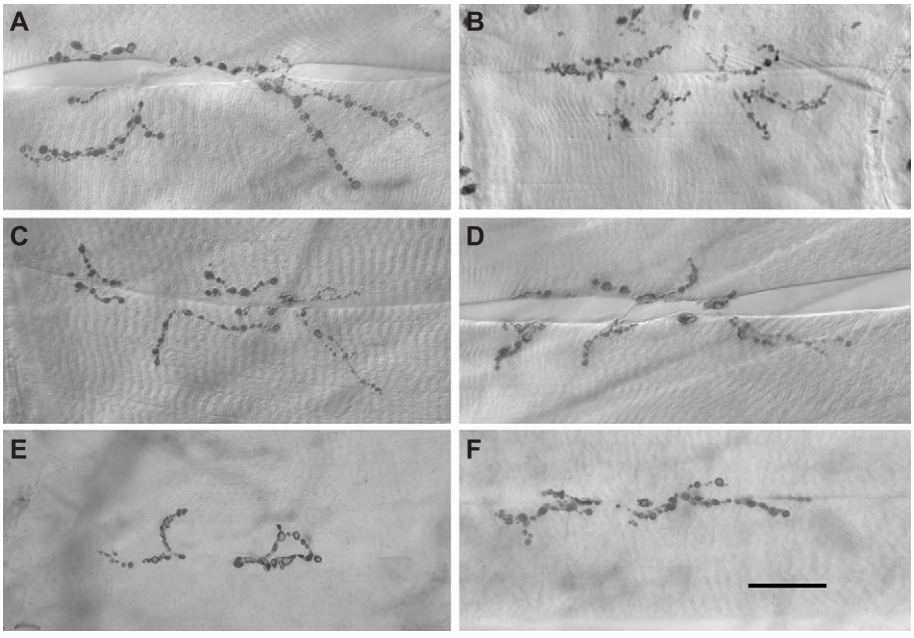

Fig. 5. Structure of NMJs on muscles 6 and 7 in w^1; cn^1, bw^1, dgs^{B19} mutant larvae following pre- and postsynaptic expression of wild-type Gsα (*UAS-GsW24*). (A) CS, control; (B–D), w^1; cn^1, bw^1, dgs^{B19} mutant larvae in which wild-type Gsα is expressed in the CNS and muscles using B185-GAL4 (w^1; cn^1, bw^1, dgs^{B19}, *GAL4-B185/*cn^1, bw^1, dgs^{B19}; +/*UAS-GsW24*) (B); CNS using *elav*-GAL4 (w^1; cn^1, bw^1, dgs^{B19}; *elav-GAL4/UAS-GsW24*) (C); or muscles using C57-GAL4 (w^1; cn^1, bw^1, dgs^{B19}; *C57-GAL4/UAS-GsW24*) (D). The UAS-Gsα transgene does not effect synaptic structure in w^1; cn^1, bw^1, dgs^{B19} larvae in the absence of a GAL4 driver (w^1; cn^1, bw^1, dgs^{B19}; +/*UAS-GsW24*) (E). Expression of a related Gα protein, UAS-Giα, in either nerve (*elav*-GAL4) (w^1; cn^1, bw^1, dgs^{B19}; *elav-GAL4/UAS-GiW11*) (F) or muscle (w^1, *MHC82-GAL4*; cn^1, bw^1, dgs^{B19}; +/*UAS-GiW11*) (data not shown) also does not rescue the synaptic defects observed in dgs^{B19} mutants. Synaptic boutons were identified and quantified following staining with antibodies directed against *Drosophila* synaptotagmin. Scale bar = 50 μm.

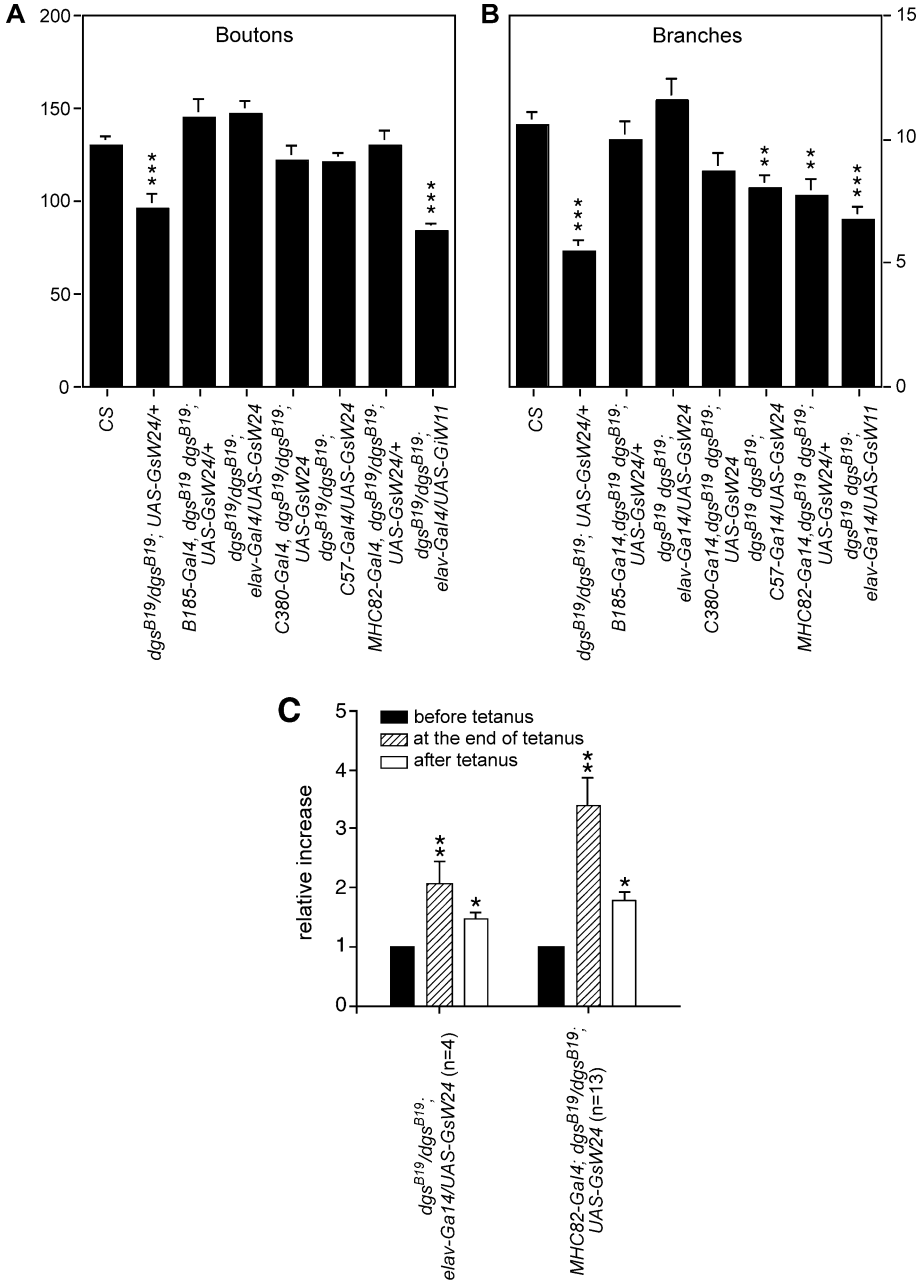

Fig. 6. Quantitation of the number of boutons and branches on muscles 6 and 7 in w^1; cn^1, bw^1, dgs^{B19} mutant larvae following pre- and postsynaptic expression of wild-type Gsα and assessment of rescue of synaptic function. (A) Quantitation of numbers of boutons and (B) the extent of synaptic arborization following expression of Gsα in nerve and muscle (w^1; cn^1, bw^1, dgs^{B19}, *GAL4-B185/*cn^1, bw^1, dgs^{B19}; +/*UAS-GsW24*), in the CNS (w^1; cn^1, bw^1, dgs^{B19}; *elav-GAL4/UAS-GsW24*), in motor neurons (w^1 *C380-GAL4*; cn^1, bw^1, dgs^{B19}; +/*UAS-GsW24*), or in muscle (w^1; cn^1, bw^1, dgs^{B19}; *C57-GAL4/UAS-GsW24* and w^1 *MHC82-GAL4*; cn^1, bw^1, dgs^{B19}; +/*UAS-GsW24*). The UAS-Gsα transgene does not effect the number of boutons and branches in w^1; cn^1, bw^1, dgs^{B19} larvae in the absence of a GAL4 driver (w^1; cn^1, bw^1, dgs^{B19}; +/*UAS-GsW24*) (data not shown). Expression of a related Gα protein, Giα, in nerve (w^1; cn^1, bw^1, dgs^{B19}; *elav*-GAL4/*UAS-GiW11*) also will not rescue the synaptic defects observed in dgs^{B19} mutant larvae. Statistical comparisons are to values observed in wild-type (CS) larvae; asterisks indicate $*p < 0.05$, $**p < 0.01$, $***p < 0.001$; $n = 15–20$ hemisegments. (C) Summary of the results of tetanic stimulation in larvae in which wild-type Gsα (UAS-Gs) is expressed in the CNS alone using *elav*-GAL4 or muscles alone using MHC82-GAL4 (genotypes as above). Three columns for each set correspond to the mean amplitude of 10 consecutive synaptic currents before tetanus (solid column), at the end of tetanus (hatched column), and immediately after tetanus (unshaded column). The mean amplitudes during tetanus and after tetanus were normalized to that before tetanus; compare to Fig. 2F, which shows results obtained in similar experiments for dgs^{B19} homozygotes and controls. Asterisks indicate that the values are significantly different from controls ($*p < 0.05$, $**p < 0.01$).

type larvae using these GAL4 drivers did not significantly alter synaptic arborization or bouton numbers when compared with controls (data not shown).

We also assessed whether restricted pre- and/or postsynaptic expression of Gsα using these GAL4 drivers was sufficient to rescue the lethality associated with the *dgs* mutations. While B185-GAL4-driven expression of wild-type Gsα in organisms carrying *dgs*-null mutations was not able to rescue the embryonic lethality associated with these mutations (data not shown), expression of Gsα using this driver was able to rescue the late larval–pupal lethality associated with the hypomorphic dgs^{B19} mutation. Moreover, restricted expression of Gsα in nerve or muscle alone did not provided for rescue to adults as was possible with the B185-GAL4 driver (data not shown). These results indicate that the ability of restricted wild-type Gsα expression to rescue the lethality associated with the hypomorphic dgs^{B19} mutant must depend on residual Gsα activity in other tissues, and rescue requires simultaneous expression in both pre- and postsynaptic cells.

NMJ defects present in dgs^{B19} larvae are not due to released βγ

The amino acid change introduced by the dgs^{B19} mutation (I373F) alters a C-terminal residue in a domain of Gsα essential for interaction with receptors but outside N-terminal regions of the protein, which have been shown in crystal structures to coordinate βγ subunits (Sprang, 1997). These considerations make it unlikely that the neuromuscular phenotypes present in dgs^{B19} larvae are due to the release or presence of unbound βγ subunits that are then free to artifactually activate downstream processes. However, since βγ subunits are potent mediators of signal transduction in heterotrimeric G protein pathways, we directly tested their involvement in the generation of the NMJ phenotypes present in dgs^{B19} larvae. We used the GAL4-UAS systems to drive the expression of an additional Gα protein, *Drosophila* Giα, to bind (i.e., "soak up") βγ subunits that might be released as a consequence of the dgs^{B19} mutation and to test whether the rescue observed in the case of Gsα was specific for this α-subunit. Similar approaches have been used in mammalian systems to demonstrate the βγ dependence of specific signaling processes (e.g., Faure et al., 1994; Lustig et al., 1993). The results demonstrate that neither expression of Giα specifically in neurons, by use of the elav-GAL4 driver (Figs. 5F and 6A and B), nor muscles, by use of the C57-GAL4 driver (data not shown), was able to rescue the defects in synaptic arborization or bouton formation present in dgs^{B19} larvae. Expression of the Giα protein in wild-type larvae had no impact on NMJ formation or viability (data not shown). Thus, the defects in NMJ formation observed in dgs^{B19} mutant larvae cannot be attributed to inappropriate activation of βγ signaling pathways. Furthermore, rescue of the dgs^{B19} neuromuscular defects is due specifically to the expression of Gsα since expression of a related G protein α-subunit, Giα, does not rescue these defects.

Synaptic expansion mediated by increased electrical activity, cAMP, and decreased cell adhesion depend on signaling through Gsα

Existing models on the role of electrical activity, intracellular cAMP, and expression of the FASII cell adhesion molecule in regulating the growth of larval synapses are based largely on an analysis of genetic interactions between mutations affecting each of these components that individually lead to excessive synaptic expansion. Given this framework, we tested the idea that synaptic overgrowth observed in these mutant backgrounds is partly or entirely dependent on normal Gsα activity by examining NMJ formation in larvae containing the dgs^{B19} mutation in combination with mutations affecting these other pathways. Specifically, we combined the dgs^{B19} mutation with *eag*, *Sh* mutations affecting neuronal electrical activity, *dnc* and *rut* mutations affecting cAMP levels, and a *fasII*

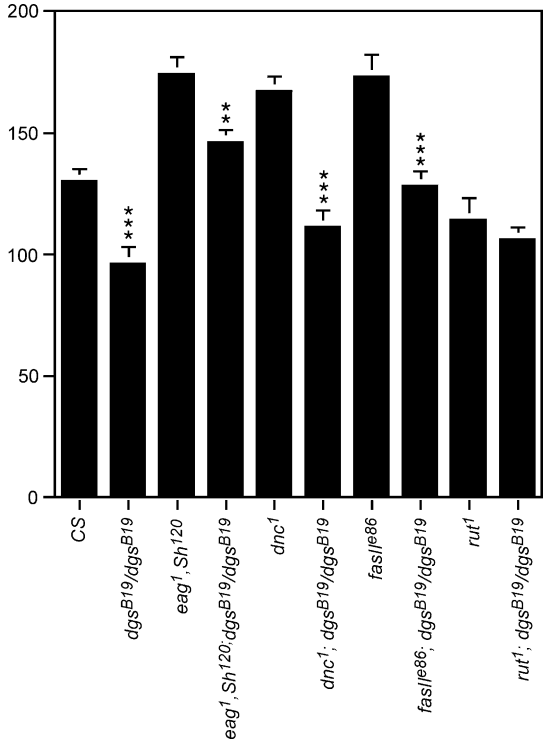

Fig. 7. Synaptic overgrowth associated with eag^1, Sh^{120}/Y double mutants and dnc^1/Y, or $fasII^{e86}/Y$ mutations is suppressed in the presence of the cn^1, bw^1, dgs^{B19} mutation. CS = cantons, ($dgs^{B19}/dgs^{B19} = cn^1$, bw^1, dgs^{B19}), (eag^1, $Sh^{120} = eag^1$, Sh^{120}/Y), (eag^1, Sh^{120}; $dgs^{B19}/dgs^{B19} = eag^1$, Sh^{120}/Y; $dgsB^{19}/dgsB^{19}$), ($dnc^1 = dnc^1/Y$), (dnc^1; $dgs^{B19}/dgs^{B19} = dnc^1/Y$; dgs^{B19}/dgs^{B19}), ($fasII^{e86} = fasII^{e86}/Y$), ($fasII^{e86}$; $dgs^{B19}/dgs^{B19} = fasII^{e86}/Y$; dgs^{B19}/dgs^{B19}), ($rut^1 = rut^1/Y$), (rut^1; $dgs^{B19}/dgs^{B19} = rut^1/Y$; dgs^{B19}/dgs^{B19}). Asterisks indicate that the number of boutons is significantly lower between the mutant alone and individual mutations in combination with the dgs^{B19} mutation (*$p < 0.05$, **$p < 0.01$, ***$p < 0.001$; $n = 15–20$ hemisegments).

mutation affecting the levels of the FASII cell adhesion molecule.

As previously reported (Budnik et al., 1990; Cheung et al., 1999; Jia et al., 1993; Schuster et al., 1996b; Zhong and Wu, 1991; Zhong et al., 1992), larvae containing eag^{1}, Sh^{120} mutations, as well as individual dnc^{1} and $fasII^{e86}$ mutations all exhibited elevated bouton numbers compared to wild-type controls, while larvae containing the rut^{1} mutation showed no significant defects in synapse formation (Fig. 7). Larvae containing $fasII^{e86}$ and dgs^{B19} mutations or eag^{1}, Sh^{120}, dgs^{B19} triple mutant larvae had intermediate numbers of boutons: fewer boutons than observed in the case of each enhancing mutation alone but greater than those observed for the dgs^{B19} mutation alone. However, larvae containing both the dnc^{1} mutation and dgs^{B19} mutations (i.e., dnc^{1}, dgs^{B19} double mutants) had significantly fewer boutons than dnc^{1} mutants alone and had bouton numbers that were no different from larvae carrying the dgs^{B19} mutation alone. Likewise, the number of boutons in rut^{1}, dgs^{B19} double mutant larvae was not significantly different from that in dgs^{B19} single mutant (Fig. 7). These results are consistent with the idea that normal Gsα-mediated signaling is required to achieve the increased growth phenotypes observed in *eag Sh*, *dnc*, and *fasII* mutants alone, as expected if cAMP were in fact a key intermediate in this pathway whose level is modulated by Gsα activity.

Modulation of synaptic FasII levels by the dgs^{B19} mutation

Synaptic overgrowth observed in *eag*, *Sh* double mutants, or in *dunce* and *fasII* single mutants depends on a reduction of FasII levels at the NMJ (Schuster et al., 1996b). For example, overgrowth generated by the *eag*, *Sh*, or *dunce* mutations can be blocked by ectopic, presynaptic expression of FASII. These and other results have led to the notion that down-regulation of synaptic FASII levels is both necessary and sufficient for growth of NMJs. Given this background, we examined whether the reduced synaptic growth observed in dgs^{B19} mutants is associated with elevated levels of FASII and whether the suppression of synaptic overgrowth by the dgs^{B19} mutation in *fasII* mutants is accompanied by a corresponding elevation in the level of

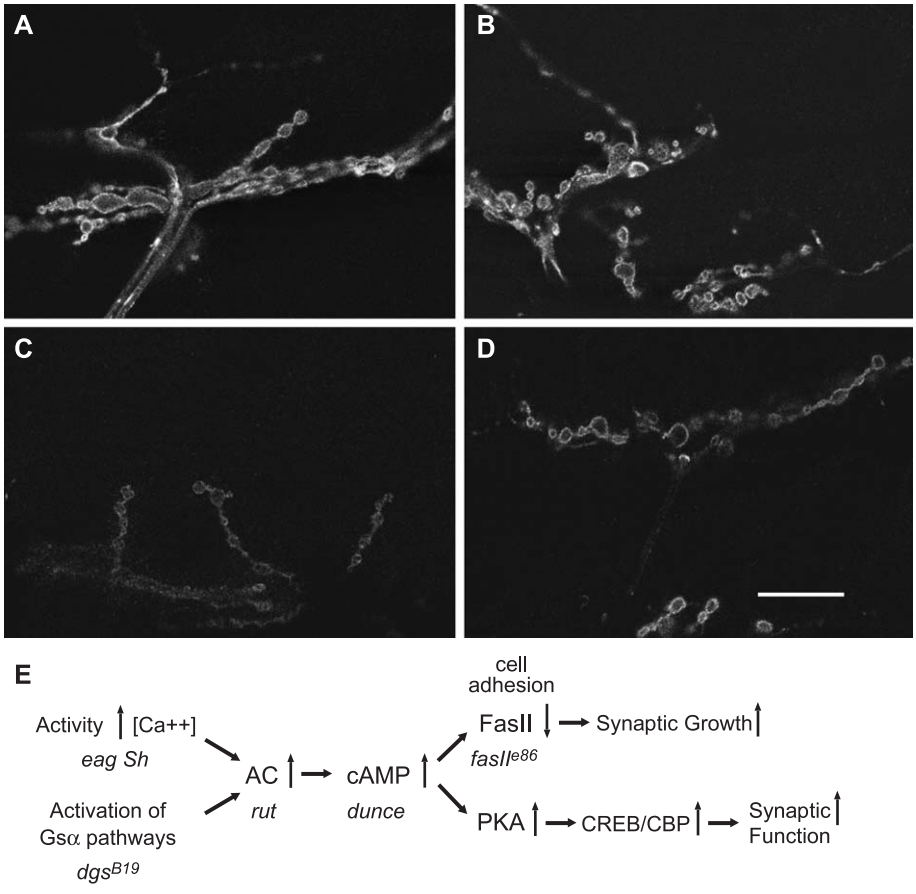

Fig. 8. Selected examples of confocal images used to compare FASII levels between control = XX; Y/dgs^{B19}/CyO (A); single dgs^{B19} mutants = XX; Y/dgs^{B19} (B); single $fasII^{e86}$ mutants = $fasII^{e86}$/Y; dgs^{B19}/CyO (C); and the double mutant $fasII^{e86}$; dgs^{B19} = $fasII^{e86}$/Y; dgs^{B19}/dgs^{B19} (D). Scale bar = 20 μm. For quantification, see Table 2. (E) Revised model of pathways by which activity- and Gsα-dependent processes, acting in parallel, modulate the activity of ACs, levels of cAMP, and subsequently synaptic growth through down-regulation of synaptic FASII levels and synaptic strength through transcriptional processes following activation of PKA/CREB/CBP. Adapted from Davis et al. (1996, 1998) and Marek et al. (2000).

Table 2
FasII staining intensity in dgs^{B19}, $fasII^{e86}$, and $fasII^{e86}$; dgs^{B19} double mutants

Genotype	*i*	*n*
dgs^{B19}/Cyo	1.00	392/9
dgs^{B19}/dgs^{B19}	1.01	359/9
$fasII^{e86}$; dgs^{B19}/Cyo	0.65	110/3
$fasII^{e86}$; dgs^{B19}/dgs^{B19}	0.83	119/3

i = index of intensity (the relative intensity compared to control tissues), see Materials and methods for details; *n* = number of varicosities/number of animals scored.

synaptic FASII (e.g., FASII levels in dgs^{B19}; $fasII^{e86}$ double mutant larvae compared to $fasII^{e86}$ mutant larvae; Fig. 7).

We assessed FASII levels in larvae of the relevant genotypes by quantitative confocal microscopy (see Materials and methods). In $fasII^{e86}$ mutant larvae (Fig 8C and Table 2), there is a substantial reduction in FASII levels (index of 0.65, Table 2) when compared to wild-type controls (Fig. 8A), leading to synaptic expansion, as previously reported (Schuster et al., 1996b). In contrast, the levels of FASII in dgs^{B19} mutant larvae (Fig. 8B) were not significantly different from that observed in controls (index of 1.01, Table 2). However, $fasII^{e86}$, dgs^{B19} mutant larvae (Fig. 8D) have intermediate levels of FASII (index of 0.83, Table 2), which were significantly different from levels in either mutant alone or in controls ($P < 0.001$). Thus, the suppression of synaptic overgrowth, observed in $fasII^{e86}$ mutant larvae, by the dgs^{B19} mutation (Fig. 7) is associated with a significant increase in FASII levels.

Discussion

The regulation of intracellular cAMP through Ca^{2+} regulation of Ca^{2+}-calmodulin-activated ACs has been implicated in processes modulating synaptic growth and strength. The ACs responsible for activity-dependent increases in intracellular cAMP integrate signals generated both by increases in neuronal Ca^{2+} and the activation of ACs through the Gsα protein. Using genetic approaches in *Drosophila*, we have been able to show that signaling through Gsα also leads to down-regulation of the relevant CAM and consequently synaptic expansion. Since technical limitations do not permit assessment of cAMP levels during formation of NMJ, earlier work showing that *Drosophila* Gsα serves as a potent activator of ACs, both in cultured cells and in whole animals (Chyb et al., 1999; Quan et al., 1991), and that the dgs^{B19} mutation leads to deficits in cAMP (Wolfgang et al., 2001), making it logical to conclude that Gsα controls synaptic growth through modulation of the levels of cAMP.

The dgs^{B19} mutation results in reductions in the number of synaptic boutons, the extent of synaptic arborization, and altered plastic properties of synaptic transmission at larval NMJs; deficits that are largely, if not completely, returned to control levels by transgenes encoding the wild-type *dgs* gene (Figs. 1 and 2). Mutant larvae have impaired synaptic transmission similar to that observed in larvae carrying mutations in the *rut* gene; facilitation during high-frequency tetanic stimulation and PTP is markedly reduced. These results are consistent with a model in which activation of ACs in wild-type larvae by Gsα-dependent processes contributes to the generation of cAMP in synaptic terminals required for the recruitment of synaptic vesicles from the reserve pool and the facilitation of transmission during high-frequency stimulation (Kuromi and Kidokoro, 2000; Renstrom et al., 1997). Although the number of boutons was found to be significantly decreased in dgs^{B19} homozygotes, the amplitude of evoked synaptic currents was not significantly different than controls. Thus, some compensatory change is elicited in response to the dgs^{B19} mutation that maintains the strength of synaptic transmission in spite of decreased numbers of synaptic boutons, perhaps through increases in the size of the readily releasable pool, a change in the probability of release, or an increase in the number of release sites per bouton.

Immunolocalization of Gsα at the EM level verified that Gsα is localized within synapses and is highly enriched in postsynaptic regions within the SSR, with lower levels present presynaptically (Fig. 3C). Complementary pre- and postsynaptic localization of Gsα within synapses was confirmed by restricted expression of epitope-tagged forms of Gsα (Figs. 3D and E). Colocalization at the light level of Gsα and FASII revealed the presence of Gsα in both periactive and active zones (Chang and Balice-Gordon, 2000; Sone et al., 2000). Moreover, Gsα localization appeared not to be altered by mutations in proteins, which serve to localize protein complexes at NMJs. Thus, Gsα occupies synaptic subdomains associated with both synaptic transmission and synaptic growth, localized either directly or indirectly via as yet unidentified organizing molecules.

We have used genetic interactions between the dgs^{B19} mutation and mutations that affect cAMP levels to assess whether cAMP is the target of Gsα-dependent signaling during synaptic growth. Our results show that the synaptic expansion observed in *eag*, *Sh* double, and *dnc* single mutants is suppressed in dgs^{B19} backgrounds (Fig. 7), as it is in *rut* mutant background (Cheung et al., 1999; Schuster et al., 1996b; Zhong et al., 1992), and as predicted if Gsα-dependent signaling plays a role in regulating overall synaptic cAMP levels. In contrast, synaptic defects observed in dgs^{B19} larvae were not enhanced in larvae carrying mutations in the *rut* gene. It is possible that more than one AC isoform may be activated by Gsα during synaptic growth (as indicated earlier, all isoforms of AC identified so far are stimulated by the GTP-bound Gsα, and the *Drosophila* genome potentially encodes up to seven AC isoforms; Cann and Levin, 1998), and the combined activation of these ACs through Gsα and Ca^{2+} may be required to set appropriate levels of cAMP. Indeed, elimination of the

rut AC has limited impact on the formation of larval NMJs (Cheung et al., 1999; Zhong et al., 1992). Furthermore, only mice in which the expression of both Ca^{2+}-calmodulin-regulated AC isoforms (AC1 and AC8) have been eliminated exhibit deficits in physiologic responses reflecting synaptic growth and plasticity (Wong et al., 1999). Alternatively, some proportion of the Gsα-generated signal may flow through effectors other than AC [e.g., src (Ma et al., 2000) or integrins (Meyer et al., 2000)]. However, the physiologic analysis of synaptic transmission in dgs^{B19} larvae and the epistatic interactions outlined above, together with previous results showing that *Drosophila* Gsα, serves as a potent activator of ACs both in cultured cells and in whole animals (Chyb et al., 1999; Quan et al., 1991), and that the dgs^{B19} mutation leads to deficits in cAMP strongly suggest that signaling through Gsα primarily controls synaptic cAMP levels.

To determine the contribution of pre- and postsynaptic expression of Gsα to the generation of the NMJ defects present in dgs^{B19} larvae (e.g., see Figs. 5 and 6), we used the GAL4-UAS system to drive expression of wild-type Gsα in specific patterns in third instar larvae. Simultaneous pre- and postsynaptic expression of Gsα restored synaptic arborization and bouton numbers to control levels in dgs^{B19} larvae (Fig. 6). We have also shown that expression of wild-type Gsα either pre- or postsynaptically alone was sufficient to rescue both bouton numbers and the physiologic defects present in dgs^{B19} homozygotes. Thus, pathways activated by Gsα are likely to be involved in reciprocal interactions between pre- and postsynaptic cells. Precedents for such reciprocal signaling between synaptic components abound. For example, postsynaptic modulation of PKA activity results in a reduction in quantal size that is accompanied by an increase in presynaptic quantal content. (Davis et al., 1998). Furthermore, postsynaptic overexpression of CBP, the coactivator involved in mediating the downstream transcriptional response evoked by cAMP, modulates presynaptic transmitter release (Marek et al., 2000). In addition, postsynaptic structural defects present in *discs-large* mutants (*dlg*) can be substantially rescued by restricted presynaptic expression of the wild-type dlg protein (Budnik et al., 1996). Finally, in a study primarily based in the physiologic consequences of expression of gain-of-function Gsα proteins, it was concluded that a bidirection transynaptic communication network at the *Drosophila* NMJ is based in Gsα signaling (Renden and Broadie, 2003), confirming the conclusions detailed here that the morphologic and physiologic phenotypes of the Gsα hypomorph can be similarly rescued by transgenic Gsα expression in either the presynaptic or the postsynaptic cell. However, we cannot specify the subcellular site of rescue since expression mediated by GAL4 drivers occurs throughout the target cell. Thus, for example, neuronal rescue of morphologic and physiologic phenotypes present in the Gsα hypomorph may be a response to the presence of Gsα either in dendrites, the cell body, or presynaptic terminals.

What remains to be determined are the mechanisms that underlie this bidirectional communication. The pathways by which cAMP mediates its effects in processes underlying synaptic growth need not be the same as those involved in modulation synaptic activity. Indeed, earlier studies outlined above suggest that growth and function are modulated by cAMP through genetically separable pathways. While previous studies have demonstrated that expression of specific signaling proteins (e.g., βPS integrins; Beumer et al., 1999) in both synaptic partners plays a key role in the regulation of synaptic growth, synaptic function is not strongly impacted by these pathways. However, in the case of Gsα-dependent signaling, as is the case for activity-dependent processes, synaptic growth and function appear to be both downstream of the activation of the adenylyl cyclases at play. The previous studies leading to the development of the basic model shown in Fig. 8E have demonstrated that cAMP-dependent down-regulation of FASII, required for synaptic growth, and cAMP-dependent increases in synaptic function each proceed by separable pathways following elevation of synaptic cAMP; a decrease in FASII is not in itself sufficient to alter synaptic function that requires PKA-dependent modulation of the activity of the transcription factor CREB (Davis et al., 1998). Thus, it is not surprising that Gsα-dependent signaling can affect both synaptic growth and synaptic function. In addition, the relevant cAMP-dependent pathways in presynaptic cells do not necessarily need to be the same as in postsynaptic cells.

The target of cAMP in the regulation of synaptic growth appears to be the homophilic cell adhesion molecule, FASII. Here, we show that the synaptic expansion generated by mutational reduction of FASII was suppressed when signaling through Gsα was abrogated by the dgs^{B19} mutation (Fig. 7), again as would be predicted if Gsα mediates its effects through modulation of synaptic cAMP (Schuster et al., 1996a,b). Additionally, it would be expected that suppression of $fasII^{e86}$-mediated synaptic expansion in dgs^{B19} mutant backgrounds would be reflected in the levels of FASII protein at synaptic terminals; down-regulation of FASII is considered necessary for structural expansion of the synapse. As shown in Fig. 8 and Table 2, quantitative confocal microscopy confirmed that the level of synaptic FASII protein in $fasII^{e86}$, dgs^{B19} double mutants is elevated compared to levels observed in $fasII^{e86}$ mutants alone. These results support a model whereby Gsα-dependent signaling plays an essential role in controlling FASII levels. However, FASII levels are not elevated in dgs^{B19} mutant larvae, as would also be predicted in this simple scheme (Fig. 8 and Table 2). It is possible that the localized reduction in FASII levels associated with formation of new boutons (Bailey et al., 1992, 1997; Zito et al., 1999) is impaired in dgs^{B19} mutants. While our methodology would not have detected spatially localized changes in FASII, when FASII levels are reduced throughout the nerve terminal in $fasII^{e86}$ mutants, the elevation of FASII levels in $fasII^{e86}$; dgs^{B19} double mutants become evident (Fig. 8D).

Our results are consistent then with a model in which Gsα-dependent activation of AC is a critical determinant of intracellular cAMP, along with activity-dependent processes, leading to the coordinated activation of ACs, the ensuing modulation of FASII levels required for synaptic growth, and establishment of cAMP levels required for the normal plastic properties of synaptic transmission (Fig. 8E). Thus, Gsα-dependent signaling can affect both synaptic growth and synaptic function, as can activity-dependent processes. How is Gsα activated during synaptic growth? The most parsimonious model is that Gsα is activated following ligand-dependent activation of an unidentified G protein-coupled receptor. The immediate effector(s) of cAMP in the modulation of synaptic growth has also not yet been precisely determined. In the classic scheme, Gsα-dependent elevation of cAMP results in the activation of protein kinase A (PKA); the PKA pathway has been implicated in the regulation of synaptic transmission at *Drosophila* NMJs (Davis and Goodman, 1998; Davis et al., 1996, 1998; Marek et al., 2000). One possible model would posit that cAMP-dependent down-regulation of FASII levels and the ensuing structural growth of synapses may be reflective of local changes in cAMP levels, while cAMP-dependent changes in synaptic efficacy may depend on more global changes. Spatially local changes in cAMP levels within individual cells have recently been suggested by use of indirect methods (Rich et al., 2001; Zaccolo and Pozzan, 2002). Mechanistically, these differences may be reflected in the cAMP-dependent activation of distinct populations of effectors. Recently, a cAMP-activated guanine nucleotide exchange factor for the ras protein, CNrasGEF, has been identified and shown to mediate the activation of ras following Gsα-dependent activation of ACs in mammalian cells (Pak et al., 2002; Pham et al., 2000). A CNrasGEF homolog is encoded by the *Drosophila* genome (Lee et al., 2002). The ras-mitogen-activated protein kinase cascade has also been shown to regulate synaptic growth in *Drosophila* through modulation of FASII-mediated cell adhesion (Koh et al., 2002). A speculative model would propose then that the dual actions of cAMP in regulating synaptic growth and in modulating the strength of synaptic transmission have their basis in the coordinated activation of distinct effectors. What remains to be determined then are the mechanisms that underlie the Gsα-dependent bidirectional communication demonstrated here and in other studies (Renden and Broadie, 2003) and whether mechanisms activated by cAMP in presynaptic cells are those also used by postsynaptic cells. The genetic strategies available in *Drosophila* should facilitate the identification of upstream activators of Gsα and the individual effectors of cAMP in each process.

Acknowledgments

The authors thank Drs. Philip Copenhaver and Sarah Smolik for critical review of the manuscript and Drs. Robert Renden and Kendal Broadie for communication of results before publication. This work was supported by grants from the National Institutes of Health (R01-NS42841; M.F.), from the Ministry of Education, Science, Sports and Culture of Japan (Y.K.), and Fondecyt (R.D. and P.L.). P.L. is an International Scholar of the Howard Hughes Medical Institute. CECS is a Millennium Science Institution.

References

Acharya, J.K., Labarca, P., Delgado, R., Jalink, K., Zuker, C.S., 1998. Synaptic defects and compensatory regulation of inositol metabolism in inositol polyphosphate 1-phosphatase mutants. Neuron 20, 1219–1229.

Akhter, S.A., Luttrell, L.M., Rockman, H.A., Iaccarino, G., Lefkowitz, R.J., Koch, W.J., 1998. Targeting the receptor-Gq interface to inhibit in vivo pressure overload myocardial hypertrophy. Science 280, 574–577.

Bailey, C.H., Chen, M., Keller, F., Kandel, E.R., 1992. Serotonin-mediated endocytosis of apCAM: an early step of learning-related synaptic growth in Aplysia. Science 256, 645–649.

Bailey, C.H., Kaang, B.K., Chen, M., Martin, K.C., Lim, C.S., Casadio, A., Kandel, E.R., 1997. Mutation in the phosphorylation sites of MAP kinase blocks learning-related internalization of apCAM in Aplysia sensory neurons. Neuron 18, 913–924.

Beumer, K.J., Rohrbough, J., Prokop, A., Broadie, K., 1999. A role for PS integrins in morphological growth and synaptic function at the postembryonic neuromuscular junction of *Drosophila*. Development 126, 5833–5846.

Bilder, D., Perrimon, N., 2000. Localization of apical epithelial determinants by the basolateral PDZ protein Scribble. Nature 403, 676–680.

Bilder, D., Li, M., Perrimon, N., 2000. Cooperative regulation of cell polarity and growth by *Drosophila* tumor suppressors. Science 289, 113–116.

Brand, A.H., Perrimon, N., 1993. Targeted gene expression as a means of altering cell fates and generating dominant phenotypes. Development 118, 401–415.

Brand, A.H., Manoukian, A.S., Perrimon, N., 1994. Ectopic expression in *Drosophila*. Methods Cell Biol. 44, 635–654.

Budnik, V., 1996. Synapse maturation and structural plasticity at *Drosophila* neuromuscular junctions. Curr. Opin. Neurobiol. 6, 858–867.

Budnik, V., Zhong, Y., Wu, C.F., 1990. Morphological plasticity of motor axons in *Drosophila* mutants with altered excitability. J. Neurosci. 10, 3754–3768.

Budnik, V., Koh, Y.H., Guan, B., Hartmann, B., Hough, C., Woods, D., Gorczyca, M., 1996. Regulation of synapse structure and function by the *Drosophila* tumor suppressor gene *dlg*. Neuron 17, 627–640.

Cann, M.J., Levin, L.R., 1998. Genetic characterization of adenylyl cyclase function. Adv. Second Messenger Phosphoprot. Res. 32, 121–135.

Chang, Q., Balice-Gordon, R.J., 2000. Highwire, rpm-1, and futsch: balancing synaptic growth and stability. Neuron 26, 287–290.

Cheung, U.S., Shayan, A.J., Boulianne, G.L., Atwood, H.L., 1999. *Drosophila* larval neuromuscular junction's responses to reduction of cAMP in the nervous system. J. Neurobiol. 40, 1–13.

Chyb, S., Hevers, W., Forte, M., Wolfgang, W.J., Selinger, Z., Hardie, R.C., 1999. Modulation of the light response by cAMP in *Drosophila* photoreceptors. J. Neurosci. 19, 8799–8807.

Cohen-Cory, S., 2002. The developing synapse: construction and modulation of synaptic structures and circuits. Science 298, 770–776.

Conklin, B.R., Herzmark, P., Ishida, S., Voyno-Yasenetskaya, T.A., Sun, Y., Farfel, Z., Bourne, H.R., 1996. *Carboxyl*-terminal mutations of Gq alpha and Gs alpha that alter the fidelity of receptor activation. Mol. Pharmacol. 50, 885–890.

Connolly, J.B., Roberts, I.J.H., Armstrong, J.D., Kaiser, K., Forte, M., Tully, T., O'Kane, C.J., 1996. Associative learning disrupted by impaired Gs signaling in *Drosophila* mushroom bodies. Science 274, 2104–2107.

Cooper, D.M., Karpen, J.W., Fagan, K.A., Mons, N.E., 1998. Ca(2+)-sensitive adenylyl cyclases. In: Cooper, D.M. (Ed.), Adv. Second Messenger Phosphoprot. Res., vol. 32. Lippincott-Raven, New York, pp. 23–51.

Davis, G.W., Goodman, C.S., 1998. Genetic analysis of synaptic development and plasticity: homeostatic regulation of synaptic efficacy. Curr. Opin. Neurobiol. 8, 149–156.

Davis, G.W., Schuster, C.M., Goodman, C.S., 1996. Genetic dissection of structural and functional components of synaptic plasticity. III. CREB is necessary for presynaptic functional plasticity (see comments). Neuron 17, 669–679.

Davis, G.W., Schuster, C.M., Goodman, C.S., 1997. Genetic analysis of the mechanisms controlling target selection: target-derived Fasciclin II regulates the pattern of synapse formation. Neuron 19, 561–573.

Davis, G.W., DiAntonio, A., Petersen, S.A., Goodman, C.S., 1998. Postsynaptic PKA controls quantal size and reveals a retrograde signal that regulates presynaptic transmitter release in *Drosophila*. Neuron 20, 305–315.

Delgado, R., Davis, R., Bono, M.R., Latorre, R., Labarca, P., 1998. Outward currents in *Drosophila* larval neurons: dunce lacks a maintained outward current component downregulated by cAMP. J. Neurosci. 18, 1399–1407.

Elgersma, Y., Silva, A.J., 1999. Molecular mechanisms of synaptic plasticity and memory. Curr. Opin. Neurobiol. 9, 209–213.

Faure, M., Voyno-Yasenetskaya, T.A., Bourne, H.R., 1994. cAMP and beta gamma subunits of heterotrimeric G proteins stimulate the mitogen-activated protein kinase pathway in COS-7 cells. J. Biol. Chem. 269, 7851–7854.

Gilchrist, A., Mazzoni, M.R., Dineen, B., Dice, A., Linden, J., Proctor, W.R., Lupica, C.R., Dunwiddie, T.V., Hamm, H.E., 1998. Antagonists of the receptor-G protein interface block Gi-coupled signal transduction. J. Biol. Chem. 273, 14912–14919.

Gilchrist, A., Bunemann, M., Li, A., Hosey, M.M., Hamm, H.E., 1999. A dominant-negative strategy for studying roles of G proteins in vivo. J. Biol. Chem. 274, 6610–6616.

Harris, B.A., Robishaw, J.D., Mumby, S.M., Gilman, A.G., 1985. Molecular cloning of complementary DNA for the alpha subunit of the G protein that stimulates adenylate cyclase. Science 229, 1274–1277.

Impey, S., Wayman, G., Wu, Z., Storm, D.R., 1994. Type I adenylyl cyclase functions as a coincidence detector for control of cyclic AMP response element-mediated transcription: synergistic regulation of transcription by Ca2+ and isoproterenol. Mol. Cell. Biol. 14, 8272–8281.

Jan, L.Y., Jan, Y.N., 1982. Antibodies to horseradish peroxidase as specific neuronal markers in *Drosophila* and in grasshopper embryos. Proc. Natl. Acad. Sci. U.S.A. 79, 2700–2704.

Jansen, G., Thijssen, K.L., Werner, P., van der Horst, M., Hazendonk, E., Plasterk, R.H., 1999. The complete family of genes encoding G proteins of *Caenorhabditis elegans*. Nat. Genet. 21, 414–419.

Jia, X.X., Gorczyca, M., Budnik, V., 1993. Ultrastructure of neuromuscular junctions in *Drosophila*: comparison of wild type and mutants with increased excitability. J. Neurobiol. 24, 1025–1044 (published erratum appears in J. Neurobiol., 1994 July;25(7):893–895).

Keshishian, H., Broadie, K., Chiba, A., Bate, M., 1996. The drosophila neuromuscular junction: a model system for studying synaptic development and function. Annu. Rev. Neurosci. 19, 545–575.

Koh, Y.H., Popova, E., Thomas, U., Griffith, L.C., Budnik, V., 1999. Regulation of DLG localization at synapses by CaMKII-dependent phosphorylation. Cell 98, 353–363.

Koh, Y.H., Gramates, L.S., Budnik, V., 2000. *Drosophila* larval neuromuscular junction: molecular components and mechanisms underlying synaptic plasticity. Microsc. Res. Tech. 49, 14–25.

Koh, Y.H., Ruiz-Canada, C., Gorczyca, M., Budnik, V., 2002. The Ras1-mitogen-activated protein kinase signal transduction pathway regulates synaptic plasticity through fasciclin II-mediated cell adhesion. J. Neurosci. 22, 2496–2504.

Kuromi, H., Kidokoro, Y., 2000. Tetanic stimulation recruits vesicles from reserve pool via a cAMP-mediated process in *Drosophila* synapses. Neuron 27, 133–143.

Lahey, T., Gorczyca, M., Jia, X.X., Budnik, V., 1994. The *Drosophila* tumor suppressor gene *dlg* is required for normal synaptic bouton structure. Neuron 13, 823–835.

Lee, J.H., Cho, K.S., Lee, J., Kim, D., Lee, S.B., Yoo, J., Cha, G.H., Chung, J., 2002. *Drosophila* PDZ-GEF, a guanine nucleotide exchange factor for Rap1 GTPase, reveals a novel upstream regulatory mechanism in the mitogen-activated protein kinase signaling pathway. Mol. Cell. Biol. 22, 7658–7666.

Li, H., Chaney, S., Roberts, I.J., Forte, M., Hirsh, J., 2000. Ectopic G-protein expression in dopamine and serotonin neurons blocks cocaine sensitization in *Drosophila melanogaster*. Curr. Biol. 10, 211–214.

Lustig, K.D., Conklin, B.R., Herzmark, P., Taussig, R., Bourne, H.R., 1993. Type II adenylylcyclase integrates coincident signals from Gs, Gi, and Gq. J. Biol. Chem. 268, 13900–13905.

Ma, Y.C., Huang, J., Ali, S., Lowry, W., Huang, X.Y., 2000. Src tyrosine kinase is a novel direct effector of G proteins. Cell 102, 635–646.

Marek, K.W., Ng, N., Fetter, R., Smolik, S., Goodman, C.S., Davis, G.W., 2000. A genetic analysis of synaptic development: pre- and postsynaptic dCBP control transmitter release at the *Drosophila* NMJ. Neuron 25, 537–547.

Martin, K.C., Kandel, E.R., 1996. Cell adhesion molecules, CREB, and the formation of new synaptic connections (comment). Neuron 17, 567–570.

Mathew, D., Gramates, L.S., Packard, M., Thomas, U., Bilder, D., Perrimon, N., Gorczyca, M., Budnik, V., 2002. Recruitment of scribble to the synaptic scaffolding complex requires GUK-holder, a novel DLG binding protein. Curr. Biol. 12, 531–539.

Mazzoni, M.R., Taddei, S., Giusti, L., Rovero, P., Galoppini, C., D'Ursi, A., Albrizio, S., Triolo, A., Novellino, E., Greco, G., Lucacchini, A., Hamm, H.E., 2000. A galpha(s) *carboxyl*-terminal peptide prevents G(s) activation by the A(2A) adenosine receptor. Mol. Pharmacol. 58, 226–236.

McLean, I.W., Nakane, P.K., 1974. Periodate–lysine–paraformaldehyde fixative. A new fixation for immunoelectron microscopy. J. Histochem. Cytochem. 22, 1077–1083.

Meyer, C.J., Alenghat, F.J., Rim, P., Fong, J.H., Fabry, B., Ingber, D.E., 2000. Mechanical control of cyclic AMP signalling and gene transcription through integrins. Nat. Cell Biol. 2, 666–668.

Ming, G.L., Song, H.J., Berninger, B., Holt, C.E., Tessier-Lavigne, M., Poo, M.M., 1997. cAMP-dependent growth cone guidance by netrin-1. Neuron 19, 1225–1235.

Pak, Y., Pham, N., Rotin, D., 2002. Direct binding of the beta1 adrenergic receptor to the cyclic AMP-dependent guanine nucleotide exchange factor CNrasGEF leads to Ras activation. Mol. Cell. Biol. 22, 7942–7952.

Peng, C.Y., Manning, L., Albertson, R., Doe, C.Q., 2000. The tumour-suppressor genes *lgl* and *dlg* regulate basal protein targeting in *Drosophila* neuroblasts. Nature 408, 596–600.

Pham, N., Cheglakov, I., Koch, C.A., de Hoog, C.L., Moran, M.F., Rotin, D., 2000. The guanine nucleotide exchange factor CNrasGEF activates ras in response to cAMP and cGMP. Curr. Biol. 10, 555–558.

Quan, F., Wolfgang, W.J., Forte, M.A., 1989. The *Drosophila* gene coding for the alpha subunit of a stimulatory G protein is preferentially expressed in the nervous system. Proc. Natl. Acad. Sci. U.S.A. 86, 4321–4325.

Quan, F., Thomas, L., Forte, M., 1991. *Drosophila* stimulatory G protein alpha subunit activates mammalian adenylyl cyclase but interacts poorly with mammalian receptors: implications for receptor-G protein interaction. Proc. Natl. Acad. Sci. U.S.A. 88, 1898–1902.

Rasenick, M.M., Watanabe, M., Lazarevic, M.B., Hatta, S., Hamm, H.E., 1994. Synthetic peptides as probes for G protein function. *Carboxyl*-

terminal G alpha s peptides mimic Gs and evoke high affinity agonist binding to beta-adrenergic receptors. J. Biol. Chem. 269, 21519–21525.

Renden, R.B., Broadie, K.S., 2003. Mutation and activation of G{alpha}s similarly alters pre- and postsynaptic mechanisms modulating neurotransmission. J. Neurophysiol. 89, 2620–2638.

Renstrom, E., Eliasson, L., Rorsman, P., 1997. Protein kinase A-dependent and -independent stimulation of exocytosis by cAMP in mouse pancreatic B-cells. J. Physiol. (Lond.) 502, 105–118.

Rich, T.C., Fagan, K.A., Tse, T.E., Schaack, J., Cooper, D.M., Karpen, J.W., 2001. A uniform extracellular stimulus triggers distinct cAMP signals in different compartments of a simple cell. Proc. Natl. Acad. Sci. U.S.A. 98, 13049–13054.

Roche, J.P., Packard, M.C., Moeckel-Cole, S., Budnik, V., 2002. Regulation of synaptic plasticity and synaptic vesicle dynamics by the PDZ protein Scribble. J. Neurosci. 22, 6471–6479.

Schuster, C.M., Davis, G.W., Fetter, R.D., Goodman, C.S., 1996a. Genetic dissection of structural and functional components of synaptic plasticity. I. Fasciclin II controls synaptic stabilization and growth. Neuron 17, 641–654.

Schuster, C.M., Davis, G.W., Fetter, R.D., Goodman, C.S., 1996b. Genetic dissection of structural and functional components of synaptic plasticity. II. Fasciclin II controls presynaptic structural plasticity (see comments). Neuron 17, 655–667.

Smit, M.J., Iyengar, R., 1998. Mammalian adenylyl cyclases. In: Cooper, D.M. (Ed.), Adv. Second Messenger Phosphoprot. Res., vol. 32. Lippincott-Raven, New York, pp. 1–21.

Sone, M., Suzuki, E., Hoshino, M., Hou, D., Kuromi, H., Fukata, M., Kuroda, S., Kaibuchi, K., Nabeshima, Y., Hama, C., 2000. Synaptic development is controlled in the periactive zones of drosophila synapses. Development 127, 4157–4168.

Sprang, S.R., 1997. G protein mechanisms: insights from structural analysis. Annu. Rev. Biochem. 66, 639–678.

Taussig, R., Zimmermann, G., 1998. Type-specific regulation of mammalian adenylyl cyclases by G protein pathways. In: Cooper, D.M. (Ed.), Adv. Second Messenger Phosphoprot. Res., vol. 32. Lippincott-Raven, New York, pp. 81–98.

Tejedor, F.J., Bokhari, A., Rogero, O., Gorczyca, M., Zhang, J., Kim, E., Sheng, M., Budnik, V., 1997. Essential role for *dlg* in synaptic clustering of Shaker K+ channels in vivo. J. Neurosci. 17, 152–159.

Thomas, U., Kim, E., Kuhlendahl, S., Koh, Y.H., Gundelfinger, E.D., Sheng, M., Garner, C.C., Budnik, V., 1997. Synaptic clustering of the cell adhesion molecule fasciclin II by discs-large and its role in the regulation of presynaptic structure. Neuron 19, 787–799.

Wayman, G.A., Impey, S., Wu, Z., Kindsvogel, W., Prichard, L., Storm, D.R., 1994. Synergistic activation of the type I adenylyl cyclase by Ca2+ and Gs-coupled receptors in vivo. J. Biol. Chem. 269, 25400–25405.

Wolfgang, W.J., Quan, F., Thambi, N., Forte, M., 1991. Restricted spatial and temporal expression of G-protein alpha subunits during *Drosophila* embryogenesis. Development 113, 527–538.

Wolfgang, W.J., Roberts, I.J., Quan, F., O'Kane, C., Forte, M., 1996. Activation of protein kinase A-independent pathways by Gs alpha in *Drosophila*. Proc. Natl. Acad. Sci. U.S.A. 93, 14542–14547.

Wolfgang, W.J., Hoskote, A., Roberts, I.J., Jackson, S., Forte, M., 2001. Genetic analysis of the drosophila *gsalpha* gene. Genetics 158, 1189–1201.

Wong, S.T., Athos, J., Figueroa, X.A., Pineda, V.V., Schaefer, M.L., Chavkin, C.C., Muglia, L.J., Storm, D.R., 1999. Calcium-stimulated adenylyl cyclase activity is critical for hippocampus-dependent long-term memory and late phase LTP. Neuron 23, 787–798.

Woolf, C.J., Salter, M.W., 2000. Neuronal plasticity: increasing the gain in pain. Science 288, 1765–1769.

Zaccolo, M., Pozzan, T., 2002. Discrete microdomains with high concentration of cAMP in stimulated rat neonatal cardiac myocytes. Science 295, 1711–1715.

Zhong, Y., Wu, C.F., 1991. Altered synaptic plasticity in *Drosophila* memory mutants with a defective cyclic AMP cascade. Science 251, 198–201.

Zhong, Y., Budnik, V., Wu, C.-F., 1992. Synaptic plasticity in *Drosophila* memory and hyperexcitable mutants: role of cAMP cascade. J. Neurosci. 12, 644–651.

Zito, K., Parnas, D., Fetter, R.D., Isacoff, E.Y., Goodman, C.S., 1999. Watching a synapse grow: noninvasive confocal imaging of synaptic growth in *Drosophila*. Neuron 22, 719–729.